

COMPUTATIONAL STUDIES OF BEAM DYNAMICS IN THE ETA GUN

Arthur C. Paul, V. Kelvin Neil*

A new general purpose computer code call EBQ¹⁾, has been written to simulate the beam dynamics of the ETA²⁾, find its beam emittance and evaluate effects of changes in the electrode positions and external magnetic fields. The original calculations of the ETA were made with EGUN³⁾ and yielded considerable insight into the operation of the device in the non-relativistic regime. The EBQ code was written specifically to attend to the special problems associated with high current relativistic beam propagation in axially symmetric machines possessing external 2-dimensional electric and magnetic fields. The coherent electric and magnetic self-fields of the beam must be calculated accurately. Special care has been used in the relativistic regime where a high degree of cancellation occurs between the self-magnetic and self electric forces of the beam. Additionally, EBQ can handle equally well non-relativistic problems involving multiple ion species where the space charge from each must be included in its mutual effect on the others. Such problems arise in the design of ion sources where different charge and mass states are present.

EBQ first solves Laplace's equation for the electrostatic potential u arising from the externally applied potentials. The code evaluates elliptic integrals to find the vector potential \vec{A} arising from the magnetic field coils. The electric and magnetic fields are found from the local derivatives of the potentials, we have

$$\nabla^2 u = 0, \vec{E} = -\nabla u$$

$$\vec{B} = \vec{B}_{self} + \nabla \times \vec{A},$$

and the equation of motion, (\vec{p} is the particle momentum)

$$\frac{d\vec{p}}{dt} = q(\vec{E} + \vec{v} \times \vec{B}).$$

EBQ simultaneously tracks all trajectories so as to allow for a charge deposition procedure based on inter-ray separations. The orbits are treated in Cartesian geometry (position and momentum) with z as in independent variable.

The electric self-field is calculated either by application of Gauss's law (which gives E_r only) or by the solution of Poisson's equation with a given charge distribution (i.e., a "guess" at what the distribution should be). The current enclosed by a ray, i_{IN} , is used to find the magnetic self-field,

$$\vec{B}_{self} = \frac{\mu_0 i_{IN}}{2\pi r} \hat{\theta}.$$

The charge carried by the rays is deposited on the mesh which is used on the next cycle to find the

space charge field in addition to the electrode field by solution of Poisson's equation. The axially symmetric external magnetic field is found from the local magnetic vector potential.

The next cycle is started by solving Poisson's equation in cylindrical geometry on an orthogonal rectangular mesh. The rays are then reinitialized and simultaneous tracking performed with the rays depositing charge on the lattice for use on the next cycle. This set of calculations is repeated until a predetermined number of cycles has been performed or until the first moment of the particle distribution fails to change by a predetermined amount.

Charge may be deposited on the mesh by either a standard procedure or the Neil-Cooper procedure. The standard procedure deposits the charge of a given ray on the two closest mesh points by linear interpolation. This results in the usual charge error near the axis of cylindrical symmetry. The Neil-Cooper procedure is rigorously correct in its mapping of the charge onto the lattice, even on the axis of symmetry. In this procedure, the original radial current density distribution $J_0(r_0)$ is mapped onto the lattice according to the radial distribution of the rays so as to rigorously conserve charge. This requires simultaneous integration of all orbits so that a mapping function can be generated mapping the local r distribution back to the point of origin. The charge Q between two rays to be deposited is $J(r)/v$, where v is the average velocity between consecutive rays. Rays may cross, resulting in a multi-valued contribution to the charge deposition. The charge deposited on any mesh point is the integral of the charge along the mapping function.

$$Q_n = \frac{1}{n\Delta} \int_A^B \frac{r_0 J(r_0) dr_0}{v(r_0)}$$

where Δ is the radial mesh interval, n the mesh line index, and A, B the initial radial interval bounded by the two sequential rays under consideration. The charge on axis is deposited according to

$$Q_0 = \frac{8}{\Delta^2} \int_0^{\Delta/2} \frac{r_0 J(r_0) dr_0}{v(r_0)}$$

The self magnetic field is determined from the enclosed current found from the ratio of areas of the rays as determined by the radial mapping function

$$\int B_{\theta} dl = 2\pi \mu_0 \int_0^r r J(r) dr$$

The rays can be generated by application of Childs law and Busch's theorem, or generated randomly or uniformly on a four dimensional surface, or explicitly specified from data input. The trajectories are obtained by Runge-Kutta integration of the equations of motion.

The Livermore Experimental Test Accelerator (ETA) is an induction machine operating with a pulse width of 40 nsec. Electrons are extracted from a thermionic

*Arthur C. Paul, University of California, Lawrence Berkeley Laboratory, Berkeley, California 94720.

V. Kelvin Neil, University of California, Lawrence Livermore Laboratory, Livermore, California 94550.

space charge limited cathode of 25 cm diameter by a grid operated at 85 kV positioned 1.5 cm in front of the cathode. The beam current determined from Childs law is 12,600 amperes. This current is pulled from the grid by the anode potential of 2.5 MV. The radial electric self-field of the beam is shorted in the grid-anode region by the presence of the grid electrode. The beams magnetic self-field of 200 gauss provides a self pinch focussing. On entry to the foilless anode, the radial electric field has begun to diverge the beam. External focussing solenoids are used from the entrance to the anode on ward to reduce the beam diameter to 10 cm at the end of the gun. A field equalizing electrode (called a washer) is midway between the cathode and the anode.

The simulation of the ETA was most economically accomplished by dividing the problem into three smaller problems, figures 1,2, and 3. 1) simulation of the cathode-grid region to find the self consistent electron starting conditions, 2) transport of the beam from the grid down well inside of the anode bore, and 3) an expanded region around the finite mesh grid to find the contribution of the grid wires to the beam emittance.

The figures show the electrodes, equipotential lines, electron trajectories, external solenoids coil cross-sections and the magnetic field on axis. Figure 1 shows the Pierce corrected region between the cathode and grid. Figure 2 shows the first 60 cm of the ETA. The electron trajectories were picked up from a dump at the grid found from problem 1 and have been through 10 Poisson equation ray trace iterations.

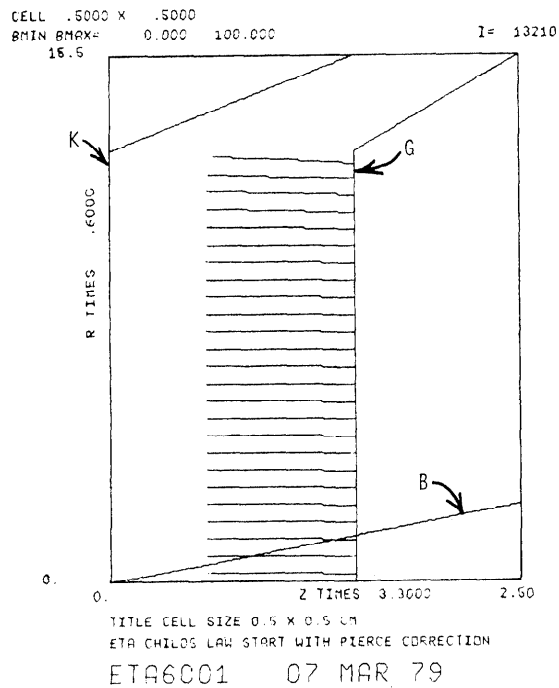


Figure 1: First section of the ETA simulation extending from the Pierce corrected cathode K, to the grid G. The plot shows the magnetic field B. The electrons originate along an equipotential line 0.6 cm before the cathode and terminate on the grid.

To find the beam emittance, including the filamentation produced by finite grid wires, a sub-problem, figure 3, is constructed extending from the cathode past the grid made up of a set of concentric wire rings to the space charged depressed 250 kV equipotential terminus of the sub-problem as determined in problem 2 shown in figure 2. 100 rays, equally spaced radially, emanating from an equipotential surface close to the cathode were found in a self-consistent iterative calculation. The construction of a mesh grid required for beam transparency and grid power dissipation produces a local radial focussing on the beam, filamentating the phase space. The grid would actually be constructed of a wire mesh, which in the limit of two dimensional axial symmetric simulation is modeled as concentric wire rings. A phase space plot of the orbits terminated at the end of this sub-problem along the curved equipotential terminus is shown in figure 4.

References

- 1) A.C. Paul, EBQ Code Transport of Space Charge Beams in Axially Symmetric Devices, UCID-8005, November, 1978.
- 2) 12 kA, 2.5 MeV electron Experimental Test Accelerator (ETA) under construction at the Lawrence Livermore Laboratory.
- 3) W.B. Herrmannsfeldt, Electron Trajectory Program, SLAC-166, September, 1973.

Acknowledgement

This work is jointly performed under the auspices of the U.S. Department of Energy by the Lawrence Livermore Laboratory under contract number W-7405-ENG-48 and ARPA order number 3718.

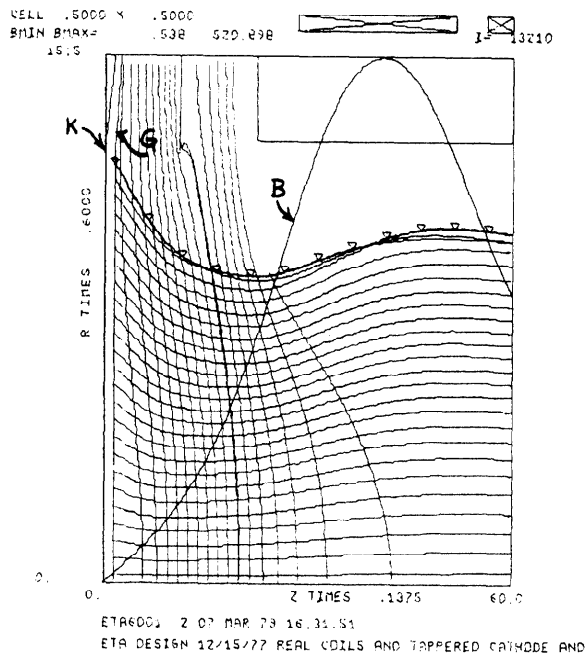
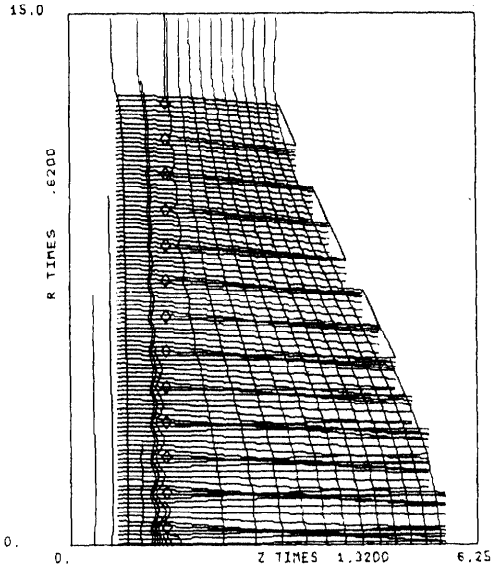


Figure 2: Second section of the ETA simulation extending from the cathode to 60 cm. The electrons are picked up from the previous problem at the grid and accelerated to 2.5 MeV.

CELL .2500 X .2500

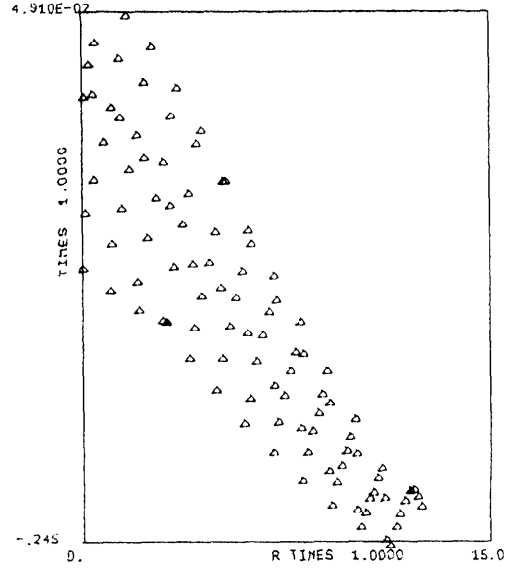
I=0.



TITLE CELL 0.25 X 0.25 CM PHASE SPACE FROM WIRE MESH
 GRID WIRE ANALYSIS ANODE AT 250 KV EQUIPOTENTIAL LIN
 X7UCI02 07 MAR 79

PR/PZ US R

RAY 6RDUP 1 I= 12142



TITLE CELL 0.25 X 0.25 CM PHASE SPACE FROM WIRE MESH
 GRID WIRE ANALYSIS ANODE AT 250 KV EQUIPOTENTIAL LINE
 X7UCI05 08 MAR 79

Figure 3: R-Z plane showing equipotential lines and electron trajectories from a non-Pierce corrected grid made of a set of concentric rings as shown. Note the local einzel lens focussing of the electron beam after passage through the grid electrode.

Figure 4: Phase space plot at the energy of 250 KeV. Rays at smaller radius passes the grid region at lower average energy due to the space charge depression of the beam and therefore received a larger radial force producing a greater phase area contribution at the smaller radii.